

Serial Intraoperative MR Imaging of Brain Shift

Arya Nabavi, M.D.¹, Peter McL. Black, M.D. Ph.D.¹, David T. Gering, M.S.⁴, Carl-Fredrik Westin, Ph.D.³, Vivek Mehta, M.D.¹, Richard S. Pergolizzi Jr., M.D.², Mathieu Ferrant, M.S.³, Simon K. Warfield, Ph.D.³, Nobuhiko Hata, Ph.D.³, Richard B. Schwartz, M.D., Ph.D.², William M. Wells III, Ph.D.⁴, Ron Kikinis, M.D.³, Ferenc A. Jolesz, M.D.³

¹ Division of Neurosurgery

² Department of Radiology

³ Surgical Planning Laboratory, Brigham and Women's Hospital, Harvard Medical School, Boston Ma

⁴ Artificial Intelligence Laboratory, Massachusetts Institute of Technology

Corresponding Author

F.A. Jolesz

Department of Radiology, L1

75 Francis Street

Brigham and Women's Hospital,

Boston, MA 02115

Tel.: (617) 732 5961

Telefax: (617) 582 6033

Email: jolesz@bwh.harvard.edu

Abstract

Introduction: The major shortcoming of image-guided navigational systems is the use of presurgically acquired image data, which does not account for intraoperative changes in brain morphology. The occurrence of these surgically induced volumetric deformations, or "brain shift", has been well established. Maximum measurements for surface and midline shifts were reported. There is no detailed analysis, however, of the changes occurring throughout the entire surgery. Intraoperative MRI provides a unique opportunity to obtain serial imaging data and characterize the time course of brain deformations during surgery. **Methods:** The vertically open-configuration (0.5 Tesla SignaSP, GE Medical Systems) intraoperative MRI system permits access to the operative field and allows multiple intraoperative image updates without the need of moving the patient. We developed volumetric display software, the "3D Slicer", which allows quantitative analysis of degree and direction of brain shift. On twenty-five patients, four or more volumetric intraoperative image acquisitions were extensively evaluated. **Results:** Serial acquisitions allow a comprehensive sequential description of the direction and magnitude of intraoperative deformations. Brain shift occurs at various surgical stages and at different regions. Surface shift occurs throughout surgery and is mainly due to gravity. Subsurface shift occurs during resection involving collapse of the resection cavity and intraparenchymal changes that are difficult to model. **Conclusions:** Brain shift is a continuous dynamic process, which

evolves differently in distinct brain regions. Therefore only serial imaging or continuous data acquisition provide consistently accurate image guidance. Furthermore only serial intraoperative MRI provides an accurate basis for the computational analysis of brain deformations, which might lead to an understanding, and eventually simulation of "brain shift" for intraoperative guidance.

Running Title: Intraoperative Brain shift

Keywords: Brain shift, computer simulation, integrated navigation, intraoperative MRI, open-configuration MRI, serial imaging

Introduction

Computer-assisted, image-guided neurosurgery is a fast growing field. There has been a continual development from frame based volumetric stereotactic tumor resections, to the wide distribution of frameless image-guided systems.

However, frameless as well as framebased stereotaxy is based on the assumption, that image space (image reflected anatomy) and physical space (patient's anatomy) can be aligned by a combination of translation and rotation (rigid transformation). This holds true only for the initial steps of the surgical procedure. With progressing surgery the shortcomings of using preoperatively acquired image data for image guidance becomes obvious. Successive changes develop and aggregate, and remain unrecognized by the navigational systems. Irrespective of the cause of intraoperative shifts or deformations (e.g. CSF drainage, tumor resection and/ or swelling) image guidance systems show a progressively outdated representation of the actual anatomy. This apparent deficiency (lack of update) diminishes the utility of currently used image guidance systems in brain surgery.

Until now mostly clinical observation and objective morphometric measurements have demonstrated substantial shifts in the range of multiple centimeters during surgical manipulations. The investigations however, reported only few time-points during surgery, and for the most part measured only the maximum brain shifts.

Some studies described the degree of shift in different regions (low, medium and large shift areas). Also, analysis of pre- and post-resection MRIs underscored such regional differences and indicated the presence of distinct compartments in the brain.

From these studies it is obvious that brain shift has a large range and is somewhat compartmentalized. Our goal has been to demonstrate that brain shift is a continuous, dynamic process, which is difficult to describe by using only few time points and hard to predict without understanding its manifestation within different regions of the brain.

The emergence of intraoperative MRI-guidance has changed the field of image-guided neurosurgery. The availability of frequent image updates not only provides correct information to the surgeon about the changing brain morphology but also permits the evaluation of some fundamental questions about the origin and course of brain deformations. Serial intraoperative

MR images with sufficient sampling rate and spatial resolution can provide the necessary data for determining the characteristic features of brain deformation. The analysis of this data may tell us how frequently we have to update the images during surgery and how accurate the morphologic information has to be in order to correct for these deformations. Therefore this data provides a basis to address the fundamental question of image-guided neurosurgery regarding the prerequisites to correct for increasing intraoperative inaccuracies due to the unavoidable "brain shift". The two opposing solutions under discussion are employing original (intraoperative imaging) or simulated (computer simulations) data amended by some intraoperative measurements to correct for intraoperative changes.

Ultrasound , Computed Tomography and Magnetic Resonance Imaging have been used for data acquisition during neurosurgical procedures. The challenge is to find a balance between the frequency of image updates, the spatial and contrast resolution of the images, and surgical access to the patient as well as the obligation to complete the surgery in a timely fashion.

Computers can potentially simulate intraoperative deformations by postulating some mechanical properties of the brain and exterior influences (e. g. gravity). Appropriately collected intraoperative information can be used to further refine these simulations, which could potentially reduce the need for intraoperative imaging. There is a potential to elastically deform (warp) pre-operative images into the intraoperative morphology. It is unclear, however, how much information is needed and how often data acquisitions should take place, to reliably drive such a calculation.

At our institution the SignaSP intraoperative 0.5 Tesla MRI (GE Medical Systems, Milwaukee, Wisconsin) allows repeated intra-operative imaging while the patient remains in scanning position throughout the procedure. This simplifies the logistics of intraoperative imaging. In this system repeated intraoperative scanning is performed on a routine basis. These images are then accessible by our integrated navigation and visualization system (3D Slicer) . Since the images are acquired intraoperatively, they represent the up-to-date situation, without the need for further processing (e.g. warping). They are unimpaired by previous deformations.

We collected a database with serial intraoperative volume acquisitions. It was our goal to investigate the time-course of intraoperative deformations, and highlight their dynamic character and regional distribution. Intraoperative imaging was performed according to a protocol and complemented by additional acquisitions according to clinical needs. This database enabled us to analyze intraoperative changes based on multiple intraoperative acquisitions and compiles the ground truth for further evaluation, development and validation of algorithms for the simulation of "brain shift".

This study presents a qualitative analysis of these serial intraoperative volumetric data.

Material and Methods

The SignaSP 0.5 Tesla intraoperative MRI, (GE Medical Systems Milwaukee, Wisconsin) was installed at the Brigham and Women's Hospital (BWH) in 1994 . Initial experiences and clinical series describe the application of this tool in neurosurgery . As of January 2000 over 340

craniotomies for tumor surgery and more than 100 brain biopsies have been performed. The characteristic feature of this intraoperative MRI is a vertically open bore (aperture 56 cm) which gives two surgeons access to the patient. The patient's head is rigidly fixed in a carbon fiber head holder (Mayfield). A flexible head-coil is placed before draping. Initial scans are taken after the patient is positioned, but before craniotomy. New images for targeting, approach and resection control are acquired as needed.

Routinely, the neuroradiologist involved specifies the 2D single or multislice imaging of the lesion and the approach. For this study we designed a volumetric 3D protocol based on a 3D SPGR (spoiled gradient pulse-sequence). These 3D volumetric data sets (Parameters: 60X2.5 mm thick slices; pixel dimensions: 2.5x0.9x0.9. mm: TR: 28.6, TE: 12.8, FOV 24x24, matrix 256x128, 1 NEX, 2.5 mm thickness/0 spacing) are acquired in addition to the conventional intraoperative scans. Scanning time is within surgically acceptable limits (3:55 min). The 3D acquisition serves simultaneously as the database for the 3D navigational interactive system the so called "3D Slicer" which can display both multiplanar and 3D reformatted images. The protocol is set to cover a minimum of 4 time-points: after positioning, as a baseline, after dural opening and initial CSF drainage, after tumor resection and finally after dural closure. Further acquisitions were obtained during resection whenever feasible. During the time of this study (October 1998 through October 1999) around 100 patients underwent craniotomies for tumor resections in the open magnet. For this study we excluded the infratentorial lesions. The protocol was employed for all other patients. The volumetric acquisition gathers data continuously during 3:55 minutes. Anything causing artifacts throughout this phase invalidates the acquisition. These cases and cases in which for surgical reasons, the entire protocol was not acquired (less than 4 volumetric acquisitions) were excluded. We included those 25 patients in the current report, who obtained a minimum of 4 or more, high-quality volumetric acquisitions SPGRs. The quality of the scan was the only inclusion criteria. The patients' age ranged between 5-67 years, the group consisted of 14 females and 11 males. The histopathological diagnosis were 23 gliomas (16 Low-grade gliomas, 7 anaplastic astrocytomas and glioblastomas) 1 epidermoid and 1 cavernous hemangioma.

The volume changes of the brain as well as the surface shift was analyzed with a toolkit developed in-house using MATLAB (Mathworks Inc.). The ventricular volume was determined by manual segmentation for the small and large lesion groups.

The qualitative analysis employed a visualization system, which was developed in collaboration with the Massachusetts Institute of Technology. The program, written in Tcl/Tk, is called "3D Slicer" .

The 3D Slicer combines image processing and 3D visualization. Furthermore this tool is integrated into the intraoperative MRI as a neuronavigation system (Nabavi et al, in preparation). The Slicer can load and display multiple data sets simultaneously. This allows the comparison of images at the same location for different stages either adjoining, or as overlay in one view. The displayed images center automatically on the same coordinate. Interspersed intraoperative images can also be displayed in this comparison (e.g. T2-w images). Although the patients were generally not moved during surgery, and the volume scans started at the same location, we wanted to ensure that there is no misalignment. This was essential for the post-processing for this study and simultaneous computational evaluations. Therefore these scans were registered employing maximization of mutual information (MMI). The registration module is fully

integrated into the 3D Slicer. This registration was employed for all patients and all intraoperative volumes. Subsequently the registered volumes are compiled in one file, permitting direct visualization of changes ([Fig 4](#)).

The MMI registration is a fully automated voxel similarity measure algorithm based on the mutual information of the acquired volumes. Thorough studies on the quality of retrospective registration algorithms included one implementation of MMI used fiducials for ground truth. Translational accuracy in MR/CT of MMI registration was achieved to 0.7 to 1.5 mm. The accuracy was dependent on the starting pose, i.e. the initial misalignment of these images, the similarity of the imaging modality (MR/PET larger errors than MR/CT) and the slice thickness.

Since the images in our study were acquired at nearly the same location and with the same modality (MR to MR), the remaining source for inaccuracies was the slice thickness at 2.5 mm (thinner slices would have prolonged the acquisition time significantly). All registration results underwent thorough visual verification, which was facilitated by the Slicer's feature of a multidisplay in 3 orthogonal planes with the capacity to overlay different scans into the same view. For the presented study none of the registrations had to be repeated. Although there was no detectable misregistration, we have to acknowledge the possibility for mismatch in our setting due to the slice thickness. Therefore the potential misalignment in our study is between 0-2.5 mm.

In addition, the 3D Slicer has functionality for semi-automated segmentation, which is used to generate 3D models and segmentations to outline regions of interest. To extract the spatial distribution of the surface shift we subtracted brain models of different stages from the baseline scan. The surface difference was automatically measured in centimeters. Visualization of these differences was accomplished by color-coding the distances in a spectrum from red to blue (where red symbolizes 0 cm, green 2.5 cm and blue 5 and more centimeter difference).

Results

We distinguished two compartments: surface and subsurface. In a single case out of 25 no brain shift was detected during the surgery; the patient had undergone radiation therapy ([Fig 1a](#)). Generally (in 20/25 patients) the surface, which comprises cortex and immediate sub-cortical white matter, shows a constant sinking in direction of gravity after craniotomy but before tumor resection ([Fig 1b](#)). If the resection cavity is smaller than the cortical opening, the surface settles during tumor resection. With the cavity larger than the cortical opening, its borders sink in, forming a crater ([Fig 2-4](#)). Only in a few cases we observed an initial outward bulging (4/25) of the surface, without previous indication of raised intracranial pressure ([Fig 1c](#)). Subsurface changes occurred in all but one case (1a), even in small superficial lesions (1b). The surface sinking propagates to the subcortical areas, and can compress the ventricular system, as the most distinct component of the subsurface structures (1b and 1d). When the weight of the overlying tissue is reduced during resection, the previously compressed areas expand ([Fig 1d](#) and [2](#)). This reversed motion directed towards the surgical site can develop a draft as far as the contra-lateral ventricle ([Fig 4](#)). In extreme cases this subsurface swelling or "rebound" can result in an obliteration of the surgical site ([Fig 1d](#)) as in 2 cases of our study.

The subsurface encompasses both the white matter and the basal ganglia and shows a clearly different deformation pattern. After dural opening the cortical sinking compresses the subsurface in direction of gravity. While the fixed dural duplicatures (falx, tentorium) remain rigid, the deformation is deflected towards the midline structures, extending over the midline. For small (< 15 ml) superficial lesions, the midline shift is hardly discernable. Since the midline structures are subject to multiple influences it is misleading, to identify motion in only one plane as maximum midline shift. The midline shift can have different directions at the same time, in relation to the most prominent force: decrease or increase of weight.

Case study

We demonstrate our approach in the case of a 39 year old woman with a right fronto-parietal oligodendroglioma (Figs 2-5). After positioning 4 successive 3D volumetric images were obtained with the SPGR sequence (Fig 2a). During resection 2D T2-w cross-sections (Fig 2b) were acquired. The navigation system, the 3D Slicer, was used for intraoperative guidance, employing the volume scan, as well as the interspersed T2-w slices.

The grayscale volumes (Fig 2a) were utilized for the initial assessment, and the subsequent post-processing. Brain, tumor and resection cavity as well as the ventricles were extracted from the volumetric image data. The brain models of the successive stages were used to calculate and color-code the surface deformations (Fig 3). To appreciate the subsurface motion grayscale cross sections from different stages were overlaid with segmented outlines of one stage. In this immediate comparison the dynamic non-linear subsurface motion becomes apparent (Fig 4). With an in-house developed software application for finite element modeling (FEM) deformation patterns can be displayed as vector fields (Fig. 5).

Morphometric image analysis

We designed specific applications for the automated measurement of brain surface shift (table 1) and brain volume changes (table 2) throughout the surgery. These measurements were calculated for all 25 patients at 4 stages (after positioning=baseline, after dural opening =1st, after resection= 2nd, and after dural closure=3rd). Three groups were arbitrarily defined according to tumor volume (less than 15 ml, 15-40 ml, 40 ml and above). The data is calculated by comparing the original data before opening (baseline) to the volume data sets during surgery (after dural opening =1st, after resection= 2nd, and after dural closure=3rd). Brain surface shift was measured in millimeters as the distance between two brain surfaces in the direction of gravity, extracted from the respective scans. Brain volume changes were calculated as the difference to the initial volume in percent.

This data was included to emphasize the wide variety of morphometric measurements, commonly given to describe intraoperative measurements.

Brain surface shift (table 1)

The calculations were made for the entire brain surface of the exposed hemisphere. The automated measurement detected the surfaces of two volume scans, and calculated the difference. The values given are the maximum shifts and their standard deviations (Fig 3 represents the surface shift as a color-coded surface model). The maximum surface shift ranges from almost no detectable shift for the smaller lesions up to 5 cm for the larger lesions. More

interesting than the overall magnitude is the tendency of the surface shift to decrease towards the end of the surgery (2nd to 3rd measurements) for all groups.

Brain volume ([table 2](#))

For all groups the brain volume increases between the end of resection (=2nd), and dural closure (=3rd). This can be due to edema, or merely expansion of previously compressed tissue ([Fig 1d](#)). In 13 out of 25 cases the brain volume increases between resection and last scan. It is noteworthy, that very large tumors (60-120 ml) show a slight volume gain after dural opening (i.e. bulging).

Ventricular volume ([table 3](#))

The ventricles were semi-automatically segmented for all 4 time points (after positioning=baseline, after dural opening =1st, after resection= 2nd, and after dural closure=3rd). Although the ventricular volume appears to be a valid indirect measurement of the midline deformation, CSF drainage and opening of the ventricular system invalidate the ventricles as a reference point for the assessment of subsurface shift. We limited the assessment of the ventricular volume to the small and large lesions. The data did not yield significant insight into subsurface motion, nor a clear distinction between the groups for small (15 ml and less) or large (40 ml and more) lesions.

Discussion

Intraoperative MRI provides imaging updates for neuronavigation but is also useful for the characterization and analysis of intraoperative brain deformations, or "brain shift". The advantage of the vertically open-configuration MRI is that serial imaging can be obtained, without moving the patient or interrupting the surgery for a longer period. We analyzed intraoperative MR images to characterize brain deformation during open craniotomies for tumor resection. Repeated intra-operative volumetric images of the entire brain were acquired. Software applications were developed to enable us to compare acquisitions from different stages of surgery. Both the magnitude and direction of brain displacement reflect the spatial extent and time course of deformations. Morphometric measurements substantiate the existence and magnitude of intraoperative "brain shift" (Tables [1](#), [2](#), [3](#)). Although these measurements underscore the dynamic character of intraoperative deformations, the multifactorial influences and regional differences are disregarded. Therefore they are only of limited value for a more thorough analysis of "brain shift". Only serial imaging with high spatial resolution allows the distinction of deformation patterns and reveals brain compartments with differing reactions to surgical manipulations.

Our results are consistent with the prior, more general, description of intra-operative brain deformations. Based on our serial imaging results we can corroborate studies, which describe the surface sinking following craniotomy and dural opening, but before surgical resection. Our observations however are not limited to the craniotomy opening . We document the continuation of brain surface shift well beyond the dural opening. This implies that areas not directly exposed by the craniotomy influence the extent of shift under the craniotomy. Depending on the patient

positioning, the temporal lobe shifts towards the midline, and limits other motion. The frontal lobe acts similarly, whereas the occipital and parietal lobes are the least mobile.

Ultrasound- and MRI-studies utilized easily identifiable structures, such as the clinoid process and ventricular system as landmarks for their analysis of brain deformations. Since we find the ventricular system to deform as a part of the subsurface, it is an unreliable fiducial. Skull base structures are more appropriate as reference for brain shift measurements. Volumetric MRI provides a direct visualization of all the important structures and their relative motion. This permits a more complete and thorough description of brain shifts and deformations. Our results show that intra-operative deformations follow a variable course, and may follow even reverse direction. Therefore it is impossible to describe and characterize intraoperative deformations by interpolating between two image data sets, one taken before and one at the completion of the surgery. This approach presumes a monotonous, linear connection between two isolated time-points. The exact sampling interval to correctly update intra-operative changes depends on the particular deformation pattern, which cannot be determined preoperatively. And even with multiple time points, it is difficult to capture the full magnitude of deformations. "Brain shift" tracking may require even more frequent or, if possible, continuous imaging. Newly developed and tested near-continuous intraoperative volumetric imaging provides constant image update without interrupting the flow of surgery (18). This method would be the ideal method to follow the entire course of brain deformation.

The task of intraoperative navigation for tumor resection and updating images for characterizing intraoperative brain shift are not necessarily identical. While brain shift tracking ideally would encompass continuous imaging, navigation is an interactive process, which relies on anatomic data acquired at a distinct point in time, based on the surgeon's request. Wirtz and Steinmeier utilized navigation systems in combination with MRI based on one update after tumor resection, to identify and remove residual tumor. The image update required an interruption of the surgery averaging 35-60 minutes. We have shown with serial imaging, that changes in brain morphology can occur within relatively short time (definitely within less than 60 minutes) even without major surgical manipulation. Moreover if deformation continues, miss-registration may result, and subsequently incorrect localization or targeting is possible. The information for our navigational system is updated with either volumetric data of the entire brain, or 2D data sets, confined to the surgical site. Because there is no need for patient transfer between operating and imaging site the time spent with imaging is relatively short (2-3 min for 2D, 4 minutes for 3D).

Intraoperative imaging should provide as frequent updates as technically possible, ideally with high spatial and contrast resolution. Currently various MRI systems with varying field strength are in use, either with an imaging system in permanent position, or with a moveable imaging device. Neither solution, however, allows frequent updates, near-real time nor continuous imaging and thus interrupts and may prolong the surgical procedure. 3D Ultrasound can be used during surgery, however both contrast resolution and unfamiliarity with the interpretation impedes its adequate application. Intra-operative CT does not provide the contrast resolution; furthermore cumulative radiation reduces the feasibility of frequent updates.

There are promising computer based models of brain deformation. Among these approaches (B-spline, optical flow) the finite element model (FEM) (Skrinjar, personal communication) is most extensively studied. These simulations are based on the assumption that the degree of deformation approaches a steady state. Although respectable results regarding the in vivo

simulation are reported, the data was obtained during surgeries which were less extensive (e. g. epilepsy) than the relatively large tumor resections. The models seem suitable for surface shift predictions, similar to the deformation observed for small lesions in this study. These show an almost monotonous, unidirectional motion, primarily caused by CSF drainage and gravity. Small and/ or surface lesions show good results with presently available simulations (Skrinjar, personal communication). For larger lesions, however, shift does not reach a steady state during surgery but initially dominates as surface and subsequently as subsurface deformations. Furthermore the shift is not necessarily unidirectional. Our results suggest that the subsurface motion during tumor resection is not driven by external pressure, but by the unburdening of weight and intra-parenchymal pressures.

Brain deformation can be influenced by multiple factors (anesthetics, fluid and electrolyte balance, positioning, CSF leakage, and internal brain structures such as vascular tree and white matter tracts). Basically the brain is neither a homogenous mass, nor an unstructured 3D body, but it is physically inhomogeneous and anatomically highly structured. The two major compartments, the surface and the subsurface consist of both gray and adjacent white matter. Dividing anatomically distinct, but otherwise combined structures (e.g. gray and white matter) does not facilitate computations. Even if the influence of each anatomical structure could be individually determined, their interaction demands new insight. These factors and the physiologic response of the brain to the surgical manipulation itself, make modeling of brain deformation difficult. Also, before reliable models can be generated we need to learn more about the biomechanical properties of the brain.

Nevertheless, in the absence of more precise knowledge of these influences, currently used models and simulations can be compared with actual intraoperative MRI data, as the ground truth.

Our unique database can be utilized for further simulations and more detailed analysis. We can test the performance of the computer-programs on real intraoperative data and determine what the minimum amount of information is, to make accurate calculations, as suggested by Roberts et al.

At present MRI is the only imaging modality capable of acquiring intra-operative images frequently and with acceptable spatial and contrast resolution. Newly developed, robust imaging methods, permitting continuous imaging would supply the updated image on demand, without interrupting the flow of surgery (18).

Summary

We report a comprehensive analysis of brain shift based on sequential acquisitions of intraoperative volumetric image data. We demonstrate the dynamic nature of intraoperative brain deformations. Neither morphometric measurements nor infrequently updated scans can fully describe this phenomenon. For the accurate assessment of intraoperative deformations more frequent or even continuous imaging would be necessary.

The presented data is necessary for the evaluation and characterization of brain deformations and

to test the overall utility of computer simulations. Predictive brain shift simulation algorithms can be developed, refined and validated employing our database. Our results suggest that surface deformations, which occur mainly due to CSF drainage in the direction of gravity, could be simulated correctly, with limited presurgical data, and meager intraoperative measurements (e.g. maximum surface shift under the craniotomy). It is clear, however, that tumor resection influences not only surface but also subsurface structures and therefore the description of brain deformations becomes far more complex. At present neither the knowledge of the biomechanical properties of the brain nor the capabilities of computer simulations are sufficient, to adequately predict the various deformation patterns we observed during surgery.

The need for presurgical knowledge of the biomechanical properties of the brain for computer assisted generation of deformation predictions is apparent. At present there is no substitute for the frequently repeated intraoperative update of image information for consistently accurate and reliable neuronavigation.

Acknowledgements

We wish to thank the members of the MRT-Team, who enable research, while carrying the weight of the clinical routine: Dan Kacher, Angela Kanan, Holly Isbister, Sharon Spalding, Cheryl Cahill, Chris Cussack, Jim Rosato, Wayne Lemire, Denis Sullivan and Sandra Robinson.

We thank the present and previous residents of the Division of Neurosurgery, especially Claudia H. Martin, and Thomas Moriarty (Louisville, Kentucky) for their help and encouragement. We thank Philip E. Stieg PhD MD. for his encouragement, support and patience.

Special thanks go to Samson Timoner, Sonja Bonitz, Tallal Charles Mamisch, Marco Das, Juergen Volker Anton, Carl P. Kolvenbach and Michael Kaus for their help and support. Eric Grimson has provided valuable criticism. AN was supported by the DFG (Deutsche Forschungsgemeinschaft: NA 356 1-1) and the "Harvard Center for Minimal Invasive Therapy". Further funding: P01-CA67165, P41-RR13218.

Figures:

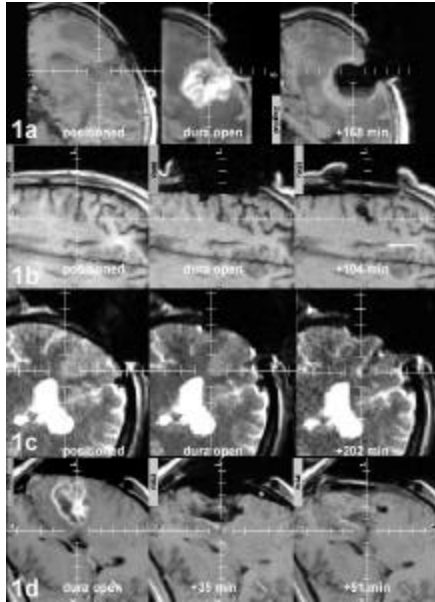


Fig. 1: The examples in this figure are from four different cases.

The images are aligned to the direction of gravity. The series show corresponding planes, acquired at the indicated successive (left to right) points in time. The hash marks begin at 1 cm from the middle and continue in 1 cm intervals. The image annotations show the elapsed time since the previous scan in minutes. There are 5-6 additional scans covering these intermittent surgical stages ([Fig. 2](#)).

a: *No brain shift*. Recurrent tumor, after irradiation: before and after contrast administration (after dural opening), and during resection (168 minutes after dural opening). The lesion is surrounded by hypointensity, interpreted as edema (T1 weighted images). There is neither a collapse of the cavity nor a detectable motion of the superior aspect of the resection cavity.

b: *Surface Sinking*. Precentral cavernous angioma. After dural opening the surface sinks constantly in direction of gravity. Towards the end of the resection it finally settles perpendicular to gravity. The surface sinking extends far beyond the craniotomy and encompasses the entire cortical surface. This sinking compresses the subjacent areas and propagates to deeper structures. The medial portion of the lateral ventricle, at the second hash mark (arrow) is continuously compressed. The midline deforms only slightly. The resection cavity is lined with surgicel (+104 minutes after dural opening).

c: *Surface Bulging*. Precentral anaplastic astrocytoma. The hyperintense lesion on T2-w images did not enhance on presurgical MRI. After positioning the sulcal pattern is well visible; there is even a small space containing CSF over the lesion. The ventricles are not compressed. After dural opening the lesion bulges out, and simultaneously compresses the surrounding sulci. The drag towards the area of least resistance propagates as far as the midline structures, and virtually pulls the respective part of the ventricular system along. Even on the final scans, after the lesion is removed (+202 min after dural opening) the sulci remain compressed and the cavity is nearly obliterated. There is no hyperintensity in the lesion's surrounding to indicate edema.

d: *Subsurface "rebound"*. Recurrent lesion after radiation. The initial image (T1 weighted) shows the lesion after dural opening. The cystic lesion enhances inhomogeneously. Well delineated to the surrounding tissue, the gross total removal was achieved within 35 minutes. The overhanging surface collapses into the cavity, resulting in surface shift (*), and the midline is deformed

towards the contralateral side. After dural closure (51 minutes later) the surface shift is less pronounced and the cavity is almost obliterated with expanding tissue. The midline structures show a detectable re-expansion.

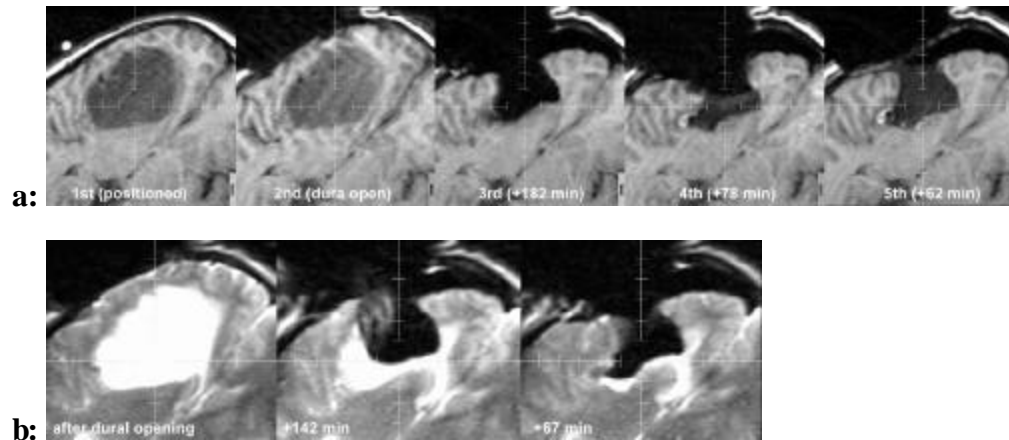


Fig. 2: Serial scanning

a: This figure shows axial planes of 5 successive 3D-volume SPGRs: 1st (after positioning); 2nd (after dural opening); 3rd (182 minutes after the 2nd); 4th (78 minutes after the 3rd) and the 5th (62 minutes after the 4th). These acquisitions were the basis for all further evaluation.

b: Interspersed T2-w images (thickness 5mm) after dural opening, 142 minutes afterwards, and 67 minutes later. The successive bulging of the medial border in correlation to the resection stage is depicted.

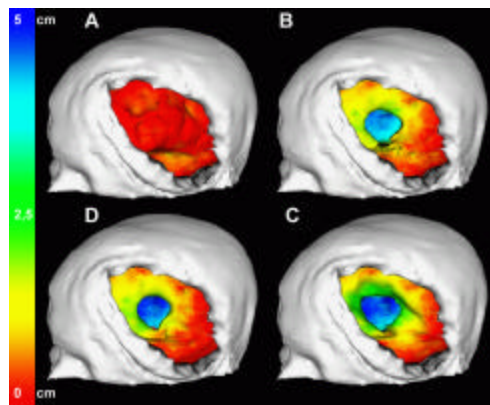


Fig. 3: Color-coded models for the evaluation of successive surface deformations.

The brain surfaces were extracted from the 3D volume SPGRs for all time points. The surface displacement from stage to stage was automatically calculated and color-coded. The color encodes depths from red (0 mm) to green (2.5 cm) to blue (5 cm). The color-coding was projected onto the model of the brain at that respective stage of the surgery.

The stages are arranged clockwise from upper left to lower left:

a) Surface motion after dural opening: mostly red depicts no notable motion at this stage.

b) Surface motion measured between stages 1st and 3rd ([Figure 2a](#)). There is a homogeneous surface sinking (yellow = 0.7 to 1.2 cm) with the largest surface shift of 1.8 cm around the edges

of the resection cavity (light green).

c) Shows the caving of the overlying cavity borders (dark green: 2.5 cm). The yellow areas (0.7 – 1.2 cm) extend further towards the parietal and temporal portions of the craniotomy.

d) After dural closure particularly the parietal and temporal areas have regained their original shape.

This stage to stage analysis underscores the difficulty in ascribing one measurement to characterize surface motion. Dynamic changes would not be represented by such singular measurements.

These color-coded models demonstrate the spatial distribution as well as the temporal course of the surface deformation. Note the changes in blue shading at the medial cavity wall.

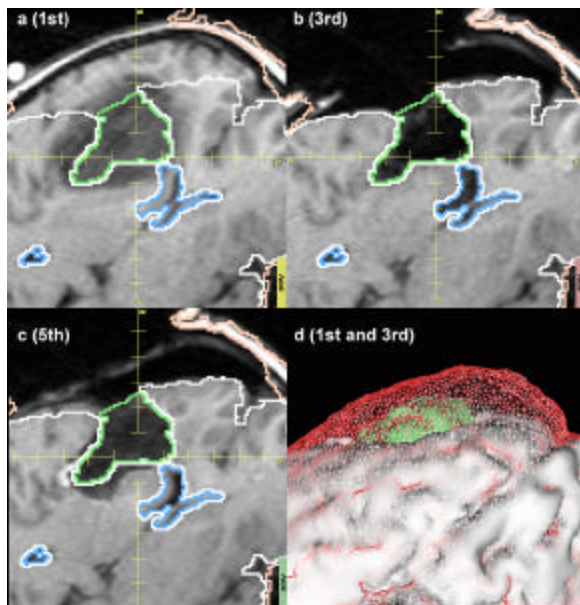


Fig. 4: Subsurface change

For the delineation of the subsurface motion we overlaid the segmented outlines of the resection cavity (green), brain (white), skin (pink) and ventricles (blue) extracted from the 3rd SPGR (b) onto the corresponding slice of the 1st (a) and 5th SPGR (c). The models in d) correspond to the brain surface at a) (red wireframe) as well as c) solid white. The tumor is displayed in its original shape, before resection.

(a) The grayscale image displays the baseline scan.

(b) The segmented data was taken from this scan (3rd SPGR). With consecutive resection the deep structures protrude into the resection cavity. This expansion pulls the subjacent areas along, resulting in a ventricular enlargement.

(c) 75 minutes later the medial wall shows a changed configuration, even without surgical manipulations. The medial wall fell back in the direction of gravity, compressing the ventricle.

(d). The 3D wire-frame shows the correlating surface motion. The tumor (solid green) is shown in its original shape, illustrating the invalidity of presurgical data to depict intraoperative changes. The white, solid brain surface model illustrates the cortical displacement. This 3D representation in combination with the 2D cuts allows the display and evaluation of intraoperative deformations in one visualization framework.

Infrequent intraoperative imaging can not show these dynamic changes adequately.

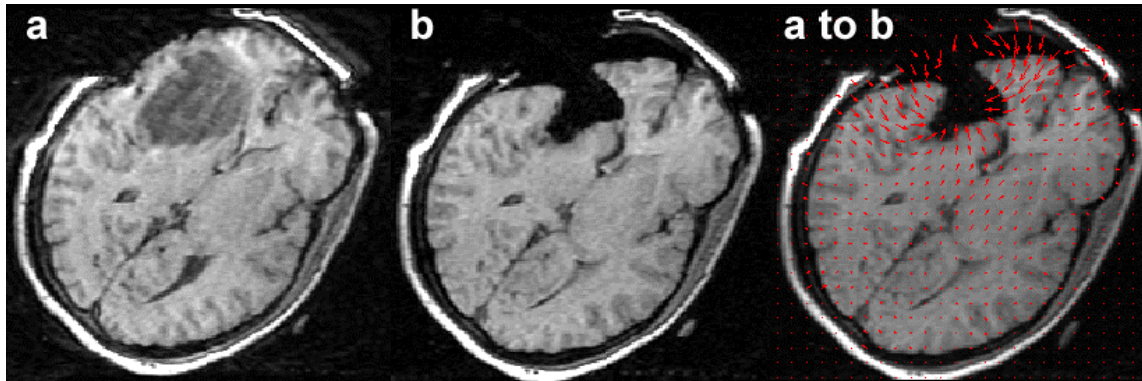


Fig. 5: Finite element modeling of intraoperative deformations.

A 3D-transformation matrix describes the elastic deformation from one stage to another. The deformation matrix is calculated as a 3-dimensional mesh for two different surgical stages (taken from [Fig 2a](#) 2nd SPGR=a and 3rd SPGR=b). The resulting 3-dimensional deformation matrix is visualized on the corresponding 2D-grayscale image as a vector field (red arrows).

Tables

Table 1: Maximum Brain Shift [mm] at 3 surgical stages

	baseline	1st	2nd	3rd
small lesions (<15 ml, n=6)	0	12.7+/-3	21.1+/-12	11.6+/-4
intermediate (15-< 40 ml, n=13)	0	15.8+/-7	23.8+/-12	12.7+/-8
large lesions (40 ml, n=6)	0	19+/- 7	37.6+/-14	11.8+/-3

positioned=baseline, after dural opening =1st, after resection= 2nd, and after dural closure=3rd.

mean and standard deviation

Table 2: Brain volume changes [%] at 3 surgical stages

	baseline	1st	2nd	3rd
small lesions (<15 ml, n=6)	100	96.2 \pm 3	88.5 \pm 6	91.5 \pm 7
intermediate (15- < 40 ml, n=13)	100	96.4 \pm 2	90.4 \pm 10	92.3 \pm 7
large lesions (40 ml, n=6)	100	97.3 \pm 4	81.8 \pm 14	85.9 \pm 8

positioned=baseline, after dural opening =1st, after resection= 2nd, and after dural closure=3rd
mean and standard deviation

Table 3: Ventricular volume changes [%] at 3 surgical stages

	baseline	1st	2nd	3rd
small lesions (<15 ml, n=6)	100	103.9 \pm 5	98.6 \pm 12	101.6 \pm 13.4
large lesions (40 ml, n=6)	100	105.5 \pm 8	90.7 \pm 24	99.1 \pm 25.8

positioned=baseline, after dural opening =1st, after resection= 2nd, and after dural closure=3rd
mean and standard deviation

References

1. Barnett GH, Kormos DW, Steiner CP, Weisenberger J: Use of a frameless, armless stereotactic wand for brain tumor localization with two-dimensional and three-dimensional neuroimaging. *Neurosurgery* 33:674-8, 1993.
2. Black PM, Alexander E, 3rd, Martin C, Moriarty T, Nabavi A, Wong TZ, Schwartz RB, Jolesz F: Craniotomy for tumor treatment in an intraoperative magnetic resonance imaging unit. *Neurosurgery* 45:423-31.
3. Black PM, Moriarty T, Alexander E, 3rd, Stieg P, Woodard EJ, Gleason PL, Martin CH, Kikinis R, Schwartz RB, Jolesz FA: Development and implementation of intraoperative magnetic resonance imaging and its neurosurgical applications. *Neurosurgery* 41:831-42.
4. Bucholz RD, McDurmont L, Smith K, Heilbrun P: Use of optical digitizer in resection of

- supratentorial tumors. Proceedings of SPIE 1894, 1993.
5. Bucholz RD, Yeh DD, Trobaugh JW, McDurmont LL, Sturm C, Baumann C, Henderson JM, Levy A, Kressman P: The correction of stereotactic inaccuracy caused by brain shift using an intraoperative ultrasound device. Springer. Grenoble, FR. 459-466. 1997.
 6. Butler WE, Piaggio CM, Constantinou C, Niklason L, Gonzalez RG, Cosgrove GR, Zervas NT: A mobile computed tomographic scanner with intraoperative and intensive care unit applications. *Neurosurgery* 42:1304-10.
 7. Collignon A, Vandermeulen D, Suetens P, Marchal G: 3D multi-modality medical image registration using feature space clustering. in N. Ayache (ed): *Computer Vision, Virtual Reality and Robotics in Medicine*. Berlin, Springer Verlag, 1995, 195-204.
 8. Dickhaus H, Ganser KA, Staubert A, Bonsanto MM, Wirtz CR, Tronnier VM, Kunze S: Quantification of brain shift effects in MRI images. Chicago. Proceedings of the 19th Annual International Conference of the IEEE:1997.
 9. Dorward NL, Alberti O, Velani B, Gerritsen FA, Harkness WF, Kitchen ND, Thomas DG: Postimaging brain distortion: magnitude, correlates, and impact on neuronavigation. *J Neurosurg* 88:656-62, 1998.
 10. Ferrant M, Warfield S, Nabavi A, Jolesz FA, Kikinis R: Registration of 3D Intraoperative MR Images of the Brain Using a Finite Element Biomechanical Model. in (ed): *MICCAI 2000*. Pittsburgh, Springer, 2000, in print.
 11. Fitzpatrick JM, Hill DL, Shyr Y, West J, Studholme C, Maurer CR, Jr.: Visual assessment of the accuracy of retrospective registration of MR and CT images of the brain. *IEEE Trans Med Imaging* 17:571-85, 1998.
 12. Gering DT, Nabavi A, Kikinis R, Grimson WEL, Hata N, Everett P, Jolesz FA, Wells WM: An integrated visualization system for surgical planning and guidance using image fusion and interventional imaging. in C. Taylor and A. Colchester (ed): *MICCAI'99*. Cambridge, UK, Springer, 1999, 809-819.
 13. Hall WA, Liu H, Martin AJ, Pozza CH, Maxwell RE, Truwit CL: Safety, Efficacy, and functionality of high-field strength interventional magnetic resonance imaging for neurosurgery. *Neurosurgery* 46:632-42, 2000.
 14. Hata N, Nabavi A, Wells WM, 3rd, Warfield SK, Kikinis R, Black PM, Jolesz FA: Three-dimensional optical flow method for measurement of volumetric brain deformation from intraoperative MR images. *J Comput Assist Tomogr* 24:531-8, 2000.
 15. Hill DL, Maurer CR, Jr., Maciunas RJ, Barwise JA, Fitzpatrick JM, Wang MY: Measurement of intraoperative brain surface deformation under a craniotomy. *Neurosurgery* 43:514-26.
 16. Jodicke A, Deinsberger W, Erbe H, Kriete A, Boker DK: Intraoperative three-dimensional ultrasonography: an approach to register brain shift using multidimensional image processing. *Minim Invasive Neurosurg* 41:13-9, 1998.
 17. Jolesz FA: 1996 RSNA Eugene P. Pendergrass New Horizons Lecture. Image-guided procedures and the operating room of the future. *Radiology* 204:601-12, 1997.
 18. Kacher DF, Maier SE, Mamata H, Mamata Y, Nabavi A, Jolesz FA: Motion robust imaging for continuous intraoperative MRI. ISMRM 8th Scientific Meeting and Exhibition, Denver, CO, 2000 p. 1330 (abstr), 2000.
 19. Kelly PJ: Computer-assisted stereotaxis: new approaches for the management of intracranial intra-axial tumors. *Neurology* 36:535-41, 1986.
 20. Lunsford LD: A dedicated CT system for the stereotactic operating room. *Appl Neurophysiol*

45:374-8, 1982.

21. Matula C, Rossler K, Reddy M, Schindler E, Koos WT: Intraoperative computed tomography guided neuronavigation: concepts, efficiency, and work flow. *Comput Aided Surg* 3:174-82, 1998.
22. Maurer CR, Jr., Hill DL, Martin AJ, Liu H, McCue M, Rueckert D, Lloret D, Hall WA, Maxwell RE, Hawkes DJ, Truwit CL: Investigation of intraoperative brain deformation using a 1.5-T interventional MR system: preliminary results. *IEEE Trans Med Imaging* 17:817-25, 1998.
23. Miga MI, Paulsen KD, Lemery JM, Eisner SD, Hartov A, Kennedy FE, Roberts DW: Model-updated image guidance: initial clinical experiences with gravity- induced brain deformation. *IEEE Trans Med Imaging* 18:866-74, 1999.
24. Miller K, Chinzei K: Constitutive modelling of brain tissue: experiment and theory. *J Biomech* 30:1115-21, 1997.
25. Okudera H, Kyoshima K, Kobayashi S, Sugita K: Intraoperative CT scan findings during resection of glial tumours. *Neurol Res* 16:265-7, 1994.
26. Paulsen KD, Miga MI, Kennedy FE, Hoopes PJ, Hartov A, Roberts DW: A computational model for tracking subsurface tissue deformation during stereotactic neurosurgery. *IEEE Trans Biomed Eng* 46:213-25, 1999.
27. Pena A, Bolton MD, Whitehouse H, Pickard JD: Effects of brain ventricular shape on periventricular biomechanics: a finite-element analysis. *Neurosurgery* 45:107-16.
28. Roberts DW, Hartov A, Kennedy FE, Miga MI, Paulsen KD: Intraoperative brain shift and deformation: a quantitative analysis of cortical displacement in 28 cases. *Neurosurgery* 43:749-58; discussion 758-60, 1998.
29. Roberts DW, Miga MI, Hartov A, Eisner S, Lemery JM, Kennedy FE, Paulsen KD: Intraoperatively updated neuroimaging using brain modeling and sparse data. *Neurosurgery* 45:1199-206.
30. Roberts DW, Strohbehn JW, Hatch JF, Murray W, Kettenberger H: A frameless stereotaxic integration of computerized tomographic imaging and the operating microscope. *J Neurosurg* 65:545-9, 1986.
31. Rubino GJ, Farahani K, McGill D, Van de Wiele B, Villablanca JP, Wang-Mathieson A: Magnetic resonance imaging-guided neurosurgery in the magnetic fringe fields: the next step in neuronavigation. *Neurosurgery* 46:643-54, 2000.
32. Schenck JF, Jolesz FA, Roemer PB, Cline HE, Lorensen WE, Kikinis R, Silverman SG, Hardy CJ, Barber WD, Laskaris ET, Dorri B, Newman RW, Holley CE, Collick BD, Dietz DP, Mack DC, Ainslie MD, Jaskolski PL, Figueira MR, vom Lehn JC, Souza SP, Dumoulin CL, Darrow RD, Peters RL, Rohling KW, Watkins RD, Eisner DR, Blumenfeld SM, Vosburgh KG: Superconducting open-configuration MR imaging system for image-guided therapy. *Radiology* 195:805-14, 1995.
33. Schwartz RB, Hsu L, Wong TZ, Kacher DF, Zamani AA, Black PM, Alexander E, 3rd, Stieg PE, Moriarty TM, Martin CA, Kikinis R, Jolesz FA: Intraoperative MR imaging guidance for intracranial neurosurgery: experience with the first 200 cases. *Radiology* 211:477-88, 1999.
34. Seifert V, Zimmermann M, Trantakis C, Vitzthum HE, Kuhnel K, Raabe A, Bootz F, Schneider JP, Schmidt F, Dietrich J: Open MRI-guided neurosurgery. *Acta Neurochir* 141:455-64, 1999.
35. Shalit MN, Israeli Y, Matz S, Cohen ML: Intra-operative computerized axial tomography. *Surg Neurol* 11:382-4, 1979.
36. Steinmeier R, Fahlbusch R, Ganslandt O, Nimsky C, Buchfelder M, Kaus M, Heigl T, Lenz

- G, Kuth R, Huk W: Intraoperative magnetic resonance imaging with the magnetom open scanner: concepts, neurosurgical indications, and procedures: a preliminary report. *Neurosurgery* 43:739-47.
37. Suhm N, Dams J, van Leyen K, Lorenz A, Bendl R: Limitations for three-dimensional ultrasound imaging through a bore-hole trepanation. *Ultrasound Med Biol* 24:663-71, 1998.
38. Sutherland GR, Kaibara T, Louw D, Hoult DI, Tomanek B, Saunders J: A mobile high-field magnetic resonance system for neurosurgery. *J Neurosurg* 91:804-13, 1999.
39. Trobaugh JW, Richard WD, Smith KR, Bucholz RD: Frameless stereotactic ultrasonography: method and applications. *Comput Med Imaging Graph* 18:235-46, 1994.
40. Tronnier VM, Wirtz CR, Knauth M, Lenz G, Pastyr O, Bonsanto MM, Albert FK, Kuth R, Staubert A, Schlegel W, Sartor K, Kunze S: Intraoperative diagnostic and interventional magnetic resonance imaging in neurosurgery. *Neurosurgery* 40:891-900, 1997.
41. Watanabe E, Watanabe T, Manaka S, Mayanagi Y, Takakura K: Three-dimensional digitizer (neuronavigator): new equipment for computed tomography-guided stereotaxic surgery. *Surg Neurol* 27:543-7, 1987.
42. Wells WM, 3rd, Viola P, Atsumi H, Nakajima S, Kikinis R: Multi-modal volume registration by maximization of mutual information. *Med Image Anal* 1:35-51, 1996.
43. West J, Fitzpatrick JM, Wang MY, Dawant BM, Maurer CR, Jr., Kessler RM, Maciunas RJ, Barillot C, Lemoine D, Collignon A, Maes F, Suetens P, Vandermeulen D, van den Elsen PA, Napel S, Sumanaweera TS, Harkness B, Hemler PF, Hill DL, Hawkes DJ, Studholme C, Maintz JB, Viergever MA, Malandain G, Woods RP: Comparison and evaluation of retrospective intermodality brain image registration techniques. *J Comput Assist Tomogr* 21:554-66, 1997.
44. Wirtz CR, Tronnier VM, Bonsanto MM, Knauth M, Staubert A, Albert FK, Kunze S: Image-guided neurosurgery with intraoperative MRI: update of frameless stereotaxy and radicality control. *Stereotact Funct Neurosurg* 68:39-43, 1997.
45. Zamorano L, Kadi AM, Dong A: Computer-assisted neurosurgery: simulation and automation. *Stereotact Funct Neurosurg* 59:115-22, 1992.
46. Zinreich SJ, Tebo SA, Long DM, Brem H, Mattox DE, Loury ME, vander Kolk CA, Koch WM, Kennedy DW, Bryan RN: Frameless stereotaxic integration of CT imaging data: accuracy and initial applications. *Radiology* 188:735-42, 1993.